

Planar Detonation Wave Initiation in Large-Aspect-Ratio Channels

S. I. Jackson*, J. M. Austin[†] and J. E. Shepherd[‡]

California Institute of Technology, Pasadena, CA 91125

Accepted for publication in the AIAA Journal, May 2006

Introduction

Planar detonation waves are often created in narrow rectangular channels to more easily visualize the cellular structure of gaseous detonation waves.¹⁻⁶ Typically, these detonation waves are initiated from a single high energy source requiring several kilojoules of input energy, such as a strong spark or exploding wire that creates a spherically or cylindrically expanding wave. This wave is then diffracted until its radius of curvature is significantly larger than the channel height, at which point it is approximated as planar.

Often a planar wave is desired in an insensitive mixture that is not able to support the aforementioned diffraction process. In this situation, the wave can be initiated and diffracted in a more sensitive gas that is separated from the insensitive mixture by a thin diaphragm. Once the wave has diffracted to an approximately planar shape, it ruptures the diaphragm and enters the insensitive gas as a planar wave. Typically the diffraction process requires tens of channel heights for the wave to diffract to an approximately planar shape. In cases where a high energy source is required for initiation, an overdriven wave is often created that requires several more channel heights to relax to a stable velocity. In large channels, the distance required to generate a planar wave can grow impractically long for facilities with limited space.

In this study, two initiator designs are presented that are able to form planar detonations with low input energy in large-aspect-ratio channels over distances corresponding to only a few channel heights. The initiators use a single spark and an array of small channels to shape the detonation wave. The first design, referred to as the static initiator, is simple to construct as it consists of straight channels which connect at

*Postdoctoral Scholar, Los Alamos National Laboratory, Los Alamos, NM 87545, Member AIAA

[†]Professor, Aerospace Engineering, University of Illinois, Urbana, IL 61801, Member AIAA

[‡]Professor, Aeronautics, Caltech MC 105-50, Pasadena, CA 91125, Member AIAA

right angles. However, it is only able to create planar waves using mixtures that can reliably detonate in its small-width channels. An improved design, referred to as the dynamic initiator, is capable of detonating insensitive mixtures using an oxy-acetylene gas slug injected into the initiator shortly before ignition, but is a more complex design. The two versions are presented below, including an overview of their design and operation. Design drawings of each initiator are available elsewhere.⁷ Finally, photographs and pressure traces of the resulting planar waves generated by each device are shown.

Initiator Design

The planar initiators are based on wave-shaping techniques used with condensed-phase explosive work at Los Alamos National Laboratory during the 1960s that ensured uniform travel times for a series of wavelets propagating from a common initiation point to an exit plane. Little work on this topic was published during that period; however, a paper by Busco⁸ contains a review of classical wave-shaping techniques.

Basic Concept

The static and dynamic planar initiators shape a detonation wave from a single initiation point into a linear distribution of wavefronts. This distributed front forms the planar detonation wave. The technique is best illustrated by describing the operation of the static initiator (Fig. 1), which consists of a main channel with secondary channels that branch off of the main channel at 90° angles. All secondary channels terminate on a unique line and exhaust into a common test-section area. The channel geometry is such that all paths from the spark point to the channel-termination line are of equal length. Thus, a detonation wave initiated in the main channel and traveling at a constant velocity would spread through the secondary channels to emerge simultaneously at the exit plane and coalesce to form a quasi-planar front.

The advantage of creating the planar wave in this fashion, rather than from a single, diffracting source, can be observed by modeling the wave merging process in a two-dimensional space with Huygens' principle, which assumes that the detonation wave propagates at a constant velocity in a direction normal to the wave front. In this case, initiation from a single source (Fig. 2) located along the centerline of a channel of height h will create a cylindrically expanding wave. When the wave radius r_s is greater than $h/2$, the deviation from planarity Δ_s of the wavefront is

$$\Delta_s = r_s - \sqrt{r_s^2 - \frac{h^2}{4}}. \quad (1)$$

Alternatively, approximating the wavelets emerging from the secondary channels of the initiator as a linear

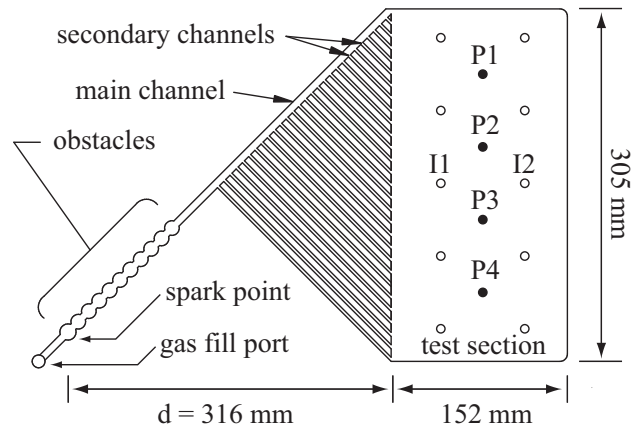


Figure 1. Channel geometry of the static initiator. In the test section, pressure transducer and ionization probe locations are indicated by filled and hollow circles respectively.

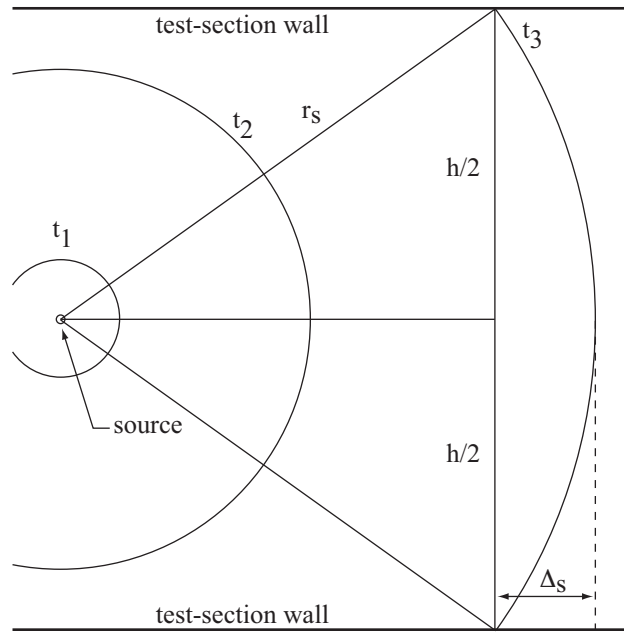


Figure 2. Wave front geometry at three different times t_i resulting from a single point source.

distribution of sources spaced apart by a distance s along a line (Fig. 3) will create a series of expanding waves which will merge to form a single, rippled front. For this distributed source, the wavefront deviation Δ_d is a function of the distributed wave radius r_d and s ,

$$\Delta_d = r_d - \sqrt{r_d^2 - \frac{s^2}{4}}. \quad (2)$$

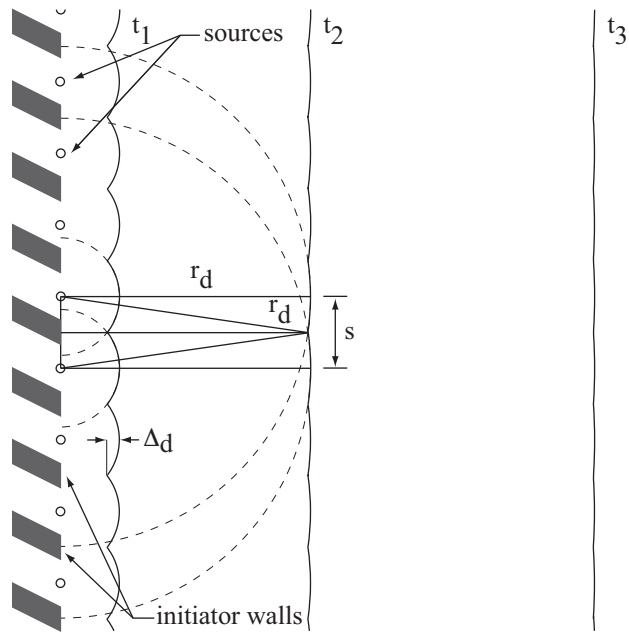


Figure 3. Wave front geometry at three different times resulting from a linear distribution of sources spaced apart by a distance s . The parameter d is shown in Fig. 1.

The effectiveness of each initiation geometry can now be evaluated by considering the distance required to generate a wave of a given wavefront deviation from the planar case. If the source spacing s is less than the channel height h for the planar initiator, the wavefront deviations in the distributed source geometry will be less than those of the single source case. However, the distance d between the spark point and the channel-termination line that is required to generate the distributed source spacing must also be added to r_d when determining the distance required for this concept. For example, on the static initiator discussed below, s was 7.6 mm, h was 305 mm, and d was 316 mm. Following the above analysis, the static initiator can be expected to produce wavefronts with deviations of 0.1 mm at the pressure transducer row (375 mm away from the spark point). In comparison, the wavefront deviation for a single, cylindrically-diffracting source at a distance of 375 mm would be 32.4 mm. In order for the single-source wavefront to achieve a deviation similar to that of the static initiator, the wave would need to travel over 150 m.

In reality, the wave propagation is expected to differ from the above model. First, wavelets emerging from the initiator are not point sources, but rather planar waves of finite dimensions. Second, the detonation velocity is not constant, decreasing during wave diffraction and increasing during wavelet merging. Finally, the waves must experience additional diffraction as they expand into a three-dimensional space, although the gradual expansion of the test section width was intended to mitigate this effect. These nonideal effects are of limited significance, however, as the wavefront deviation of the static initiator was experimentally measured to be less than 1.0 mm.

Static Initiator

The main channel of the static initiator (Fig. 1) had a $9.5 \text{ mm} \times 9.5 \text{ mm}$ square cross-section and a length of 431 mm. The head of the main channel contained a gas fill port. Just downstream of the fill port, a spark plug was located next to a series of obstacles that were milled into the main channel to promote deflagration-to-detonation transition (DDT). The secondary channels each had a $5.1 \text{ mm} \times 5.1 \text{ mm}$ cross-section and were spaced 2.54 mm apart.

The secondary channels exhausted into a test section that was 152 mm long and 305 mm high. The test section contained a ramp near the secondary channel exhaust that enlarged the channel width from 5.1 mm to 19.1 mm over a distance of 38.1 mm. The substrate containing the channels and test section was aluminum. The top surface of the initiator was covered with a 28.6-mm-thick, optically transparent, polycarbonate window. In order to create a gas-tight seal on the top surface of each channel and prevent the detonation wavelets from jumping to other channels, a 1.0-mm-thick Teflon gasket was sandwiched between the polycarbonate window and the planar initiator to seal the top of the device and transmit chemiluminescence. Both surfaces of the Teflon were covered with a thin layer of RTV silicone sealant.

The test section contained one row of four PCB 113A26 pressure transducers and two rows of ionization probes⁷ that were used to detect the planarity of the detonation wave in the test section. The row of transducers was located 59.1 mm from the channel-termination line while the ionization probe rows were located 30.5 mm and 87.6 mm respectively from the termination line. Data from the pressure transducers and the ionization probes were collected using two Tektronics TDS 460 oscilloscopes and were processed using Labview software. The sampling rate of the oscilloscopes was 2.5 MHz. An intensified CCD (Princeton Instruments ITE/ICCD-576) camera recorded the chemiluminescence from the combustion with a single 100 ns exposure for visual inspection of the wave shape. The pressure transducers provided the precise arrival time information of the shock wave in the test section, which allowed determination of wavefront deviations from differences in the arrival times at each transducer. The CCD camera imaged the chemiluminescence behind the wave and provided an image of the wave planarity, while the two ionization probes (one was located in the center of each ionization row) allowed the wave velocity in the center of the test section to be determined.

During testing, the device was filled with stoichiometric propane-oxygen and ethylene-oxygen mixtures with initial pressures ranging from 0.20 to 1.50 bar. Gas mixtures were prepared using the method of partial pressures and then mixed for 15 minutes in a separate vessel. A Champion REJ-38 spark plug and associated discharge system with 46 mJ of stored energy was used to ignite the combustible mixture.

For pressures above 0.50 bar, the static initiator consistently generated planar waves with deviations of less

than 1.0 mm over the 305 mm test-section height for all mixtures tested. For propane-oxygen mixtures, decreasing the pressure below 0.50 bar increased the wavefront deviations above 1.0 mm. A set of pressure traces from the experiment are shown in Fig. 4 that correspond to a wavefront deviation of 0.5 mm. While the experimentally measured value of Δ_d is slightly larger than the theoretical estimate, it is much smaller than the calculated value of Δ_s . Images of the detonation chemiluminescence from three different runs (Fig. 5) show the detonation wavelets exiting the secondary channels and merging to form a uniform, planar front that propagates across the test section.

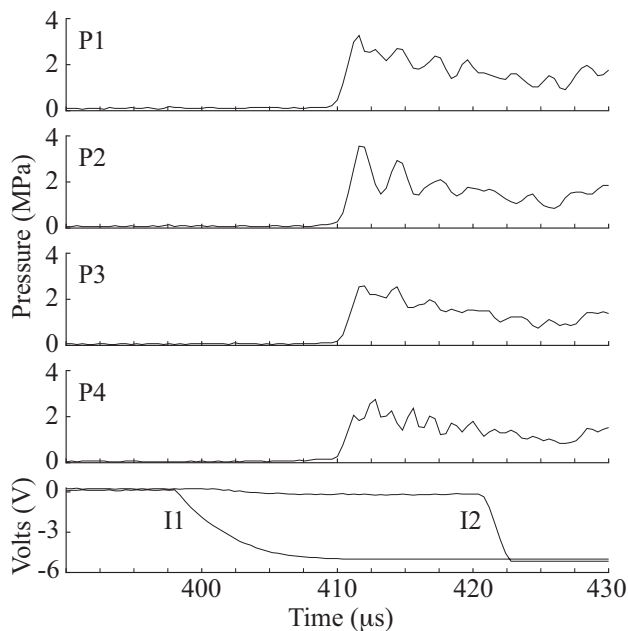


Figure 4. Pressure (P1-P4) and ionization probe data (I1 and I2) from a test with the static initiator filled with stoichiometric propane-oxygen at 1.0 bar. The difference in wave arrival times at the transducers was less than $0.2 \mu\text{s}$ and the wave speed detected from ionization probe measurements was 2551 m/s, corresponding to a wavefront deviation of 0.5 mm.

Dynamic Initiator

During testing of the static initiator, detonations in the initiator channels were found to fail if the test mixture was too insensitive to propagate in the initiator channels. In order to facilitate better performance with such test mixtures, the initiator was redesigned so that a mixture of equimolar oxygen and acetylene could be uniformly injected into the initiator channels shortly before ignition. This sensitive mixture filled the initiator channels and displaced the less sensitive test mixture, allowing stable detonation propagation in the channels.

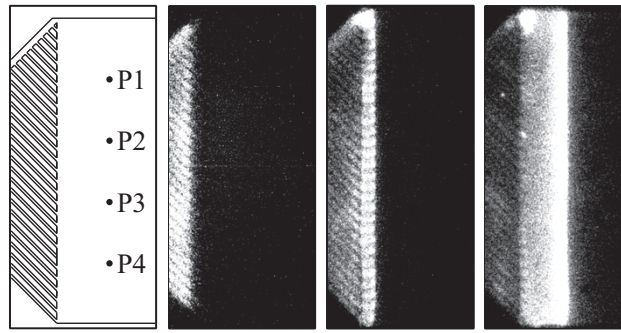


Figure 5. Static initiator results showing a schematic of the imaging area along with images taken $360 \mu\text{s}$, $370 \mu\text{s}$, and $375 \mu\text{s}$ after ignition. Each image was taken during a separate experiment. The test mixture was stoichiometric propane-oxygen at 1.0 bar.

To ensure that the sensitized gas was uniformly injected into the initiator channels, the channel geometry of the dynamic initiator was redesigned such that all channel paths had equal lengths and flow resistances (Fig. 6). Path lengths were identical due to the symmetry of the channel design along the long axis. This symmetry also lends itself to uniform flow resistance: At each channel intersection, the downstream channels branch out at similar angles (in opposite directions) and have similar channel widths. While more complicated to machine, the design also does not require detonations in the channels to turn sharp corners, which can weaken detonation waves and cause them to fail, resulting in nonideal initiator operation. The channel dimensions of the dynamic initiator are shown in Table 1.

Table 1. Dimensions for each series of dynamic initiator channels shown in Fig. 6.

Series number	Number of channels	Channel width	Arc length per channel
1	1	10.2 mm	152.4 mm
2	2	8.5 mm	115.7 mm
3	4	7.2 mm	89.4 mm
4	8	6.1 mm	53.8 mm
5	16	5.1 mm	35.6 mm

A 33.0-mm-thick plate covered the top of the dynamic initiator. Both the cover plate and the initiator were machined from aluminum and their interface was sealed with a 1.27-mm-thick copper gasket. Several bolt holes were located between the channels and sealed with O-rings, which allowed the cover plate to be securely attached to the top of the initiator and ensured that the gasket was crushed sufficiently. At the channel-termination line located at the start of the test section, the channel cross-section is $5.1 \text{ mm} \times 5.1 \text{ mm}$ and the channel spacing s at this location is 4.45 mm. The test section was 152 mm high and the width gradually expanded from the initiator channel exit height (5.1 mm) to 18 mm.

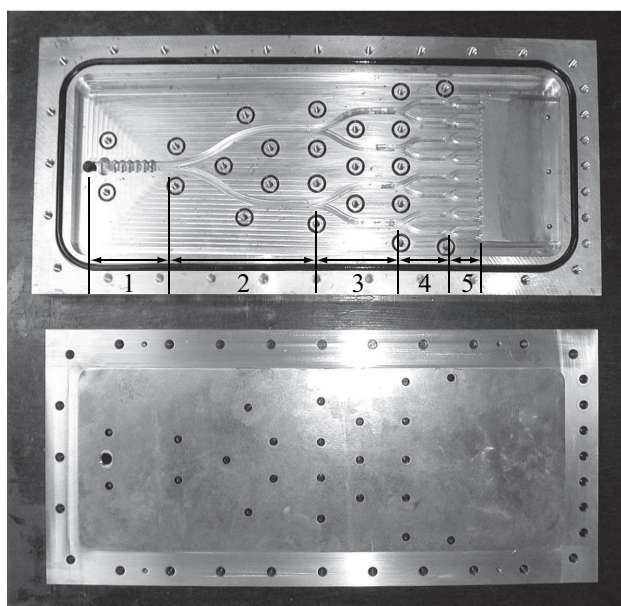


Figure 6. The dynamic planar initiator (top) and cover plate (bottom) are shown. When fully assembled, the gasket is located between the dynamic initiator and the cover plate. The numbers indicate each channel series. Note the symmetric channel design.

The test section contained three PCB model 113A26 pressure transducers located 73.7 mm from the channel-termination line. Each transducer was connected to a data acquisition system with a sampling rate of 1 MHz. For visualization of chemiluminescence, the aluminum cover plate and copper gasket shown in Fig. 6 were replaced with an optically transparent, polycarbonate cover plate and a Teflon gasket. Images were acquired with the aforementioned ICCD camera.

The gas injection system was driven by an interlocked timing circuit that controlled the injection of the equimolar acetylene-oxygen mixture into the initiator and the firing of the spark plug. In order to characterize the planarity of the waves produced by the dynamic initiator, the device was filled with air to a pressure of 0.2 bar prior to the activation of the injection system. The system then injected gas for 0.8 seconds to fill the initiator channels. Immediately after ignition, the spark plug was discharged.

Figure 7 shows the detonation propagation through the dynamic initiator. Each image is from a separate experiment and the channel orientation is the same as in Fig. 6. In the final image, the detonation wavelets in the channels have combined in the test section to form the planar detonation front. Pressure data indicate that the wave produced in the test section is planar to within 6.0 mm over the test section height of 152 mm. Using this technique, the planar initiator is able to initiate stoichiometric propane-oxygen diluted with 60% nitrogen by volume and stoichiometric ethylene-oxygen diluted with 72% nitrogen by volume.⁹ Currently, the dynamic initiator is used to create detonations for use in Caltech's Narrow Channel Facility,^{6,9} which is

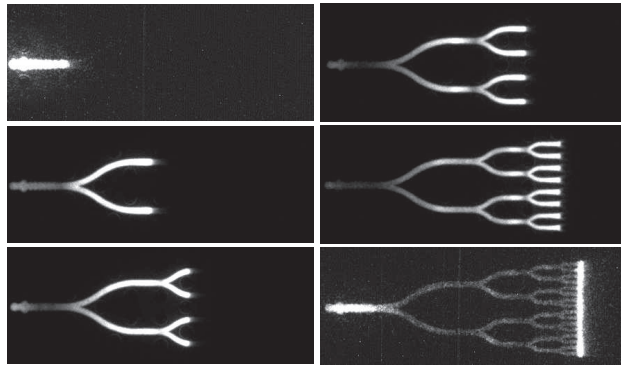


Figure 7. Chemiluminescence images from the dynamic planar initiator.

used to study the cellular structure and stability of gaseous detonation fronts.

Theoretical deviations Δ_d and Δ_s for the dynamic initiator were calculated to be 0.03 mm and 6.44 mm respectively. Thus, the experimentally measured value of Δ_d is significantly larger than the theoretical value and compares more closely to the calculated value of Δ_s . The larger wavefront deviation is attributed to flow disturbances created by the injection process, however this gas injection is necessary to prevent the wave from failing. Experimentally, it would be difficult to obtain the theoretical value Δ_s from simple diffraction in insensitive mixtures, as the expanding detonation wave would fail unless it was significantly overdriven. Also, as discussed in the introduction, an overdriven wave would require additional length to relax to a stable velocity.

Conclusions

Two initiator designs have been presented that are capable of generating planar detonation waves in channels with large aspect ratios. Both initiators create planar waves in significantly shorter distances than can be done by simply diffracting a wave from a single initiation point in a tube. The static initiator has a simple design that consists of straight channels and produces waves in a 305 mm \times 19.0 mm channel that are planar to within 1.0 mm at a distance of 375 mm away from the initiation point. However, the static initiator is only able to generate such waves in sensitive mixtures. The dynamic initiator has a more complex channel geometry and uses a gas injection system to generate planar waves in insensitive mixtures such as stoichiometric propane-oxygen diluted with 60% nitrogen by volume and stoichiometric ethylene-oxygen diluted with 72% nitrogen by volume. Waves generated with the dynamic initiator are planar to within 6.0 mm over the length of the 152 mm \times 18.0 mm test section. Modified versions of these initiators have also been used to generate toroidally imploding detonation waves.^{10, 11}

Acknowledgements

The authors are grateful for the assistance of M. Grunthaler and F. Pintgen. This work was sponsored by the Department of Defense and Army Research Office through a National Defense Science and Engineering Graduate (NDSEG) Fellowship, by the Office of Naval Research Grants “*Pulse Detonation Engines: Initiation, Propagation and Performance*,” “*Multidisciplinary Study of Pulse Detonation Engine*,” and “*Detonation Initiation by Annular Jets and Shock Waves*,” and by General Electric.

References

- ¹Voitsekhovskii, B., Mitrofanov, V., and Topchian, M. Y., “Struktura Fronta Detonastii I Gaza,” *Akad. Nauk., SSSR, Novosibirsk*, 1966, Translation available as: The Structure of a Detonation Front in Gases, Rep. FTD-MT-64-527, Foreign Technology Division, Wright-Patterson A.F.B., Ohio.
- ²Nagaishi, T., Yoneda, K., and Hikita, T., “On the Structure of Detonation Waves in Gases,” *Combustion and Flame*, Vol. 16, No. 1, 1971, pp. 35–38.
- ³Edwards, D., Hooper, G., and Meddins, R., “Instabilities in the Reaction Zones of Detonation Waves,” *Astronautica Acta*, Vol. 17, No. 4-5, 1974, pp. 475–485.
- ⁴Strehlow, R. and Crooker, A., “The Structure of Marginal Detonation Waves,” *Astronautica Acta*, Vol. 1, No. 3-4, 1974, pp. 303–315.
- ⁵Subbotin, V., “Two Kinds of Transverse Wave Structures in Multifront Detonation,” *Combustion, Explosion, and Shock Waves*, Vol. 11, No. 1, 1975, pp. 96–102.
- ⁶Austin, J., Pintgen, F., and Shepherd, J., “Reaction Zones in Highly Unstable Detonations,” *Proceedings of the Combustion Institute*, Pittsburgh, PA, 2005, pp. 1849–1857.
- ⁷Jackson, S., *Gaseous Detonation Initiation via Wave Implosion*, Ph.D. thesis, California Institute of Technology, Pasadena, CA, 2005.
- ⁸Busco, M., “Optical Properties of Detonation Waves (Optics of Explosives),” *Proceedings of the Fifth Symposium on Detonation*, Arlington, VA, 1970, pp. 513–522.
- ⁹Austin, J., *The Role of Instability in Gaseous Detonation*, Ph.D. thesis, California Institute of Technology, Pasadena, CA, 2003.
- ¹⁰Jackson, S. and Shepherd, J., “Initiation Systems for Pulse Detonation Engines,” 38th AIAA/ASME/SAE/ASEE Joint Propulsion Conference and Exhibit, July 7-10, 2002, Indianapolis, IN, AIAA 2002-3627.

¹¹Jackson, S., Grunthaner, M., and Shepherd, J., “Wave Implosion as an Initiation Mechanism for Pulse Detonation Engines,” 39th AIAA/ASME/SAE/ASEE Joint Propulsion Conference and Exhibit, July 20-23, 2003, Huntsville, Alabama, AIAA 2003-4280.